Anomalously high thermoelectric power factor in epitaxial ScN thin films

Kerdsongpanya, Sit; Van Nong, Ngo; Pryds, Nini; Žukauskaitė, Agnė; Jensen, Jens; Birch, Jens; Lu, Jun; Hultman, Lars; Wingqvist, Gunilla; Eklund, Per

Published in:
Applied Physics Letters

Link to article, DOI:
10.1063/1.3665945

Publication date:
2011

Anomalously high thermoelectric power factor in epitaxial ScN thin films

Sit Kerdsongpanya*[a], Ngo Van Nong[b], Nini Pryds[b], Agnė Žukauskaitė[a], Jens Jensen[a], Jens Birch[a], Jun Lu [a], Lars Hultman,[a] Gunilla Wingqvist[a], Per Eklund[a]

[a]Thin Film Physics Division, Department of Physics, Chemistry, and Biology (IFM), Linköping University, SE-581 83 Linköping, Sweden.

[b]Fuel Cells & Solid State Chemistry Division, Risø National Laboratory for Sustainable Energy, Technical University of Denmark, DK-4000 Roskilde, Denmark.

ABSTRACT

Thermoelectric properties of ScN thin films grown by reactive magnetron sputtering on Al_2O_3(0001) wafers are reported. X-ray diffraction and elastic recoil detection analyses show that the composition of the films is close to stoichiometry with trace amounts (~1 at.% in total) of C, O, and F. We found that the ScN thin-film exhibits a rather low electrical resistivity of ~2.94 $\mu\Omega$·m, while its Seebeck coefficient is approximately -86 μV/K at 800 K, yielding a power factor of ~2.5 x 10^{-3} W/m·K^2. This value is anomalously high for common transition-metal nitrides.

Keywords: Transition-metal nitride, Seebeck coefficient, X-ray diffraction, Electron microscopy

* Corresponding author. E-mail sitke@ifm.liu.se

Thermoelectric generators using thermoelectric materials directly convert heat into electricity by generating a potential difference in response to a temperature gradient (or vice versa). The conversion efficiency of a thermoelectric device depends on the thermoelectric figure of merit (ZT) at a certain temperature (T), where $Z = S^2/(\rho \cdot \kappa)$ and S, ρ, and κ are the Seebeck coefficient, the electrical resistivity, and the thermal conductivity, respectively. Since S, ρ, and κ are interdependent, it is a challenging task to improve ZT.[1,2] For typical thermoelectric materials, κ is dominated by the lattice thermal conductivity; the maximum ZT is then close the maximum of the parameter S^2/ρ, called the power factor. Here, we report a thermoelectric power factor of 2.5×10^{-3} W/(m·K^2) at 800 K for epitaxial ScN thin films due to a relatively high Seebeck coefficient of ~-86 μV/K with low electrical resistivity (~2.94 $\mu\Omega$·m). This is an anomalously high power factor for transition-metal nitrides and may place ScN-based materials as promising candidates for high temperature thermoelectric applications.

Transition-metal nitrides have not been commonly considered for thermoelectric applications. Yet, they are much appreciated as wear-resistant coatings and electronic contacts materials because of their thermal and mechanical stability, electrical conductivity, and chemical inertness. Like many other transition-metal nitrides, ScN has high hardness and high melting point ~2900 K.[3,4] It possesses a NaCl (B1) crystal structure with a lattice parameter of 4.521 Å. For electrical properties, theoretical studies reported that ScN is an indirect semiconductor with energy gap in the range of 0.9-1.6 eV.[5-9] Measurements on as-deposited ScN show n-type behavior[10,11] and the carrier concentration of ScN has been reported to vary from 10^{18} to 10^{22} cm^{-3} with electron mobility of 100-180 cm^{2}V^{-1}s^{-1}.[9,12-14] These numbers of the carrier concentrations span the typical ideal range for thermoelectrics[1] while retaining a high carrier mobility;[13] a fact relevant to their thermoelectric power factor reported here.

ScN films were grown onto Al_2O_3(0001) substrates using reactive magnetron sputtering in an ultrahigh vacuum chamber with a base pressure of ~10^{-7} Pa. The chamber is described elsewhere.[15] The Sc target (99.99% purity specified as the amount of Sc divided by the total rare-earth metals in the target) has a diameter of 5 cm. The substrates were one-side polished Al_2O_3(0001) wafers. Prior to deposition, the substrates were degreased in an ultrasonic bath with trichloroethylene, acetone, and isopropanol for 5 min. each, and subsequently blown dry with N_2. Before deposition, the substrates were heated in vacuum to the deposition temperature 800 °C (for 1 h for temperature stabilization and degassing). The Sc target was operated in dc mode (power-regulated) at a power of 80 W. The substrate was rotated during deposition in order to obtain uniform films. The depositions were performed in Ar/N_2 (flow ratio 87% Ar / 13% N_2) with the total gas pressure at 0.2 Pa. Structural characterization of as-deposited films was performed by X-ray diffraction (XRD) using CuK_α radiation. θ-2θ scans were measured in a Philips PW 1820 diffractometer; ϕ-scans and pole figures were measured in a Philips X'pert Materials Research Diffractometer operated with point focus, primary optics of 2 × 2 mm cross slits, and secondary optics with parallel-plate collimator. The ϕ-scan of ScN *200* peak was scanned with a fixed 2θ angle of 40.16°, a fixed tilt angle (ψ) of 54.7°, and azimuth-angle (ϕ) range 0-360° with step size 0.1°. Cross-sectional specimens for transmission electron microscopy (TEM) were prepared by gluing two pieces of the sample face to face and clamped with a Ti grid, polishing down to 50 μm thickness. Ion milling was performed in a Gatan Precision Ion Polishing System (PIPS) at Ar^+ energy of 5 kV and a gun angle of 5°, with a final polishing step with 2 kV Ar^+ energy and angle of 2°. TEM characterization was performed using a Tecnai G2 TF20UT with a field-emission gun (FEG). Compositional analysis of as-deposited film was performed by time-of-flight elastic recoil detection analysis (ToF-ERDA). Here, a 30 MeV $^{127}I^{9+}$ beam was directed to the films at an incident angle of 67.5° with respect to the surface normal, and the target recoils were detected

at an angle of 45°. The spectra was analyzed using the CONTES code for conversion to composition depth profile.[16,17] The Seebeck coefficient and in-plane electrical resistivity of the film were simultaneously measured from room temperature up to ~800 K by an ULVAC-RIKO ZEM3 system in vacuum with a low-pressure helium atmosphere. The substrate contribution to the Seebeck coefficient and electrical resistivity is negligible. Hall-effect measurements were done at room temperature in van der Pauw configuration with four symmetrical electrodes and platinum contacts bonded by gold wires to the electrodes.

Figure 1(a) shows a θ - 2θ XRD pattern from an as-deposited ScN film. The pattern shows the ScN *111* diffraction peak at a 2θ angle of 34.33° corresponding very well to ICDD PDF 45-0978 as well as the Al_2O_3(0001) substrate peak. From the *111* peak position of the ScN film, the lattice parameter was determined to be 4.51 Å. The inset of Fig. 1 shows a ϕ-scan of ScN *200* at 40.16°. The six peaks are due to diffraction from planes of the {200} family. The three-fold symmetry of the [200] orientation in a cubic crystal should give three peaks; the fact that there are six shows that there are twin-domains because of different stacking sequences in which ScN(111) can be grown on Al_2O_3(0001). The expected epitaxial relationship for the ScN(111) grown onto the Al_2O_3(0001) surface would be $<1\bar{1}0>_{ScN}||<10\bar{1}0>_{Al_2O_3}$ in-plane and $(111)_{ScN}||(0001)_{Al_2O_3}$ out of plane. However, XRD shows that the <110> directions of the ScN domains are here rotated in average ±4° compare to the $<10\bar{1}0>$ direction on the sapphire surface. This effect may be due to minimize the stresses resulting from the 17% positive mismatch between the ScN and sapphire lattices and weak interaction from second or third nearest neighbor of rhombohedral/cubic stacking.

Figure 2(a) is an overview cross-section TEM image of a typical ScN film. It can be seen that the film has columnar domains and a thickness of ~180 nm. Fig. 2(b) shows a high-resolution

image of the interface area of film and substrate. The image shows the epitaxial growth of ScN on Al_2O_3, consistent with XRD. Fig. 2(c) shows a high resolution TEM image with a lattice parameter *a* of ScN which agrees with that observed by XRD. ERDA showed that the film composition is 49.6±1.5 at.% of Sc and 49.3±1.5 at.% of N, i.e., close to stoichiometric. There are trace amounts of F, O, and C (~0.7 at.%, ~0.3 at.%, and ~0.1 at.%, respectively). The source of the fluorine is from the Sc target due to the production process. The appearance of the films is transparent orange, which indicates that the composition is close to stoichiometric.[10,12]

The thermoelectric properties of ScN are shown in Figure 3(a) and (b). At 800 K, the Seebeck coefficient is ~-86 μV/K and the in-plane electrical resistivity is ~2.94 $\mu\Omega$·m, giving a power factor of 2.5×10^{-3} W/m·K^2. By assuming the literature value for the thermal conductivity of ScN,[4] the ZT value can be estimated to ~0.2 at 800 K. This should be considered a lower limit of ZT. Even so, it is comparable to such established thermoelectric materials as polycrystalline $Ca_3Co_4O_9$.[18] In comparison with other transition-metal (like CrN), the ScN is five times larger in ZT value.[19] The measurements were performed in several cycles from room temperature to 800 K to ensure the obtained results are reproducible. Fig. 3(b) shows the repeated power factor measurement; the values are virtually identical. The diffraction pattern of the ScN was also unchanged after three cycles from room temperature to 800 K, confirming the structural stability of the ScN films in this temperature range.

The results show that our ScN films have a relatively high (negative) Seebeck coefficient for transition-metal nitrides in combination with a high electrical conductivity, resulting in a remarkably high thermoelectric power factor. In order to tentatively explain this phenomenon, we note that the conductivity is metallic-like both in magnitude and temperature-dependence.

Hall measurements at room temperature yielded an electron concentration of 1.0×10^{21} cm^3 and an electron mobility of 30.0 cm^2 V^{-1} s^{-1}. This may be due to small contamination from oxygen, fluorine or nitrogen vacancies acting as dopants to increase carrier concentration. Additionally, the impurities might cause rapidly changing features in the density of states near the Fermi level. It has been theoretically predicted that nitrogen vacancies have this role in ScN and it is reasonable that dopants could yield a similar effect.[7] Preliminary caluclations support this notion.[20] Such features in the density of states would correspond to the Mahan and Sofo prediction of the transport-distribution function that maximizes ZT.[21]

Additional samples (not shown) with higher oxygen contents (1-3 at.%) and/or substoichiometric in nitrogen, exhibited Seebeck coefficients somewhat lower, but of the same order as shown in Fig. 3(a). However, they also exhibited large difference in electrical resistivity, i.e., up to one order of magnitude higher electrical resistivity for 1-3 at.% O content than the ScN films with ~0.3 at.% O content. Hall measurements for ScN with ~1-3 at.% O show an electron concentration increase to 1.25×10^{21} - 1.75×10^{21} cm^3 and electron mobilities in the range 0.5 – 1.6 cm^2 V^{-1} s^{-1}. This may be due to either incorporation of O in ScN or formation of secondary phases, e.g., amorphous oxides. According to the Mott equation, the Seebeck coefficient is independent of mobility if the mobility is energy-independent, therefore these data are consistent with the large reduction in conductivity (due to reduced mobility) and limited reduction in Seebeck coefficient. These observations of large variation in properties emphasize the importance of impurities and defects. The only previous report on thermoelectric properties of ScN reported a relatively modest power factor for “bulk ScN” without providing any information about the samples or their purity.[22]

In conclusion, the thermoelectric properties of epitaxial ScN thin films have been studied in detail. It is possible to obtain ScN exhibiting a remarkably high power factor 2.5×10^{-3} W/(m·K^2) at 800 K which corresponds to a relatively high Seebeck coefficient of ~-86 μV/K while retaining a rather low and metallic-like electrical resistivity (~2.94 $\mu\Omega$·m). The estimated lower limit of ZT is ~0.2 at 800 K, which suggests that the ScN-based materials as candidates for high-temperature thermoelectrics application.

ACKNOWLEDGMENT

Funding from the Swedish Research Council (VR, grant number 621-2009-5258) is acknowledged.

REFERNCES

[1]G. J. Snyder and E. S. Toberer, Nat. Mater. **7**, 105 (2008).

[2]F. J. DiSalvo, Science **285**, 703 (1999).

[3]D. Gall, I. Petrov, N. Hellgren, L. Hultman, J. E. Sundgren, and J. E. Greene, J. Appl. Phys. **84**, 6034 (1998).

[4]V. Rawat, Y. K. Koh, D. G. Cahill, and T. D. Sands, J. Appl. Phys. **105**, 024909 (2009).

[5]D. Gall, M. Städele, K. Järrendahl, I. Petrov, P. Desjardins, R. T. Haasch, T.-Y. Lee, and J. E. Greene, Phys. Rev. B **63**, 125119 (2001).

[6]C. Stampfl, W. Mannstadt, R. Asahi, and A. J. Freeman, Phys. Rev. B **63**, 155106 (2001).

[7]M. G. Moreno-Armenta and G. Soto, Computational Materials Science **40**, 275 (2007).

[8]W. R. L. Lambrecht, Phys. Rev. B **62**, 13538 (2000).

[9]H. A. Al-Brithen, A. R. Smith, and D. Gall, Phys. Rev. B **70**, 045303 (2004).

[10]H. A. H. Al-Brithen, E. M. Trifan, D. C. Ingram, A. R. Smith, and D. Gall, J. Cryst. Growth **242**, 345 (2002).

[11]M. A. Moram, Z. H. Barber, and C. J. Humphreys, Thin Solid Films **516**, 8569 (2008).

[12]G. Travaglini, F. Marabelli, R. Monnier, E. Kaldis, and P. Wachter, Phys. Rev. B **34**, 3876 (1986).

[13]J. M. Gregoire, S. D. Kirby, G. E. Scopelianos, F. H. Lee, and R. B. van Dover, J. Appl. Phys. **104**, 074913 (2008).

[14]J. P. Dismukes, W. M. Yim, J. J. Tietjen, and R. E. Novak, R.C.A. Review **31**, 680 (1970).

[15]D. H. Trinh, H. Hogberg, J. M. Andersson, M. Collin, I. Reineck, U. Helmersson, and L. Hultman, J. Vac. Sci. Technol. A. **24**, 309 (2006).

[16]M. S. Janson, CONTES, Conversion of Time-Energy Spectra A Program for ERDA Data Analysis, Internal Report, Uppsala University, 2004.

[17]H. J. Whitlow, G. Possnert, and C. S. Petersson, Nucl. Instrum. Meth. B **27**, 448 (1987).

[18]N. V. Nong, N. Pryds, S. Linderoth, and M. Ohtaki, Adv. Mater. **23**, 2484 (2011).

[19]C. X. Quintela, F. Rivadulla, and J. Rivas, Appl. Phys. Lett. **94**, 152103 (2009).

[20]G. Soto, M. G. Moreno-Armenta, and A. Reyes-Serrato, arXiv:0803.3644v1[cond-mat.mtrl-sci], epublished (2008).

[21]G. D. Mahan and J. O. Sofo, Proc. Nat. Acad. Sci. USA **93**, 4436 (1996).

[22]M. Zebarjadi, Z. Bian, R. Singh, A. Shakouri, R. Wortman, V. Rawat, and T. Sands, J. Electron. Mater. **38**, 960 (2009).

FIGURE CAPTIONS

FIG 1. θ-2θ x-ray diffraction pattern from a ScN film deposited onto an Al_2O_3(0001) substrate. The inset shows a ϕ-scan plot of (solid line) the ScN *200* plane and (dot line) the Al_2O_3 $10\bar{1}4$ plane.

FIG 2. Cross-sectional TEM micrographs of a ScN film on Al_2O_3(0001) substrate in (a) overview and (b) high resolution of the film/substrate interface, and (c) high-resolution of a region in the bulk of the film.

FIG 3. (color online) Thermoelectric properties of a ScN film was measured from room temperature to 800 K, (a) Seebeck coefficient (*left*) and electrical resistivity (*right*) as functions of temperature, and (b) Power factor S^2/ρ vs. temperature from 300 – 800 K for three measured cycles.

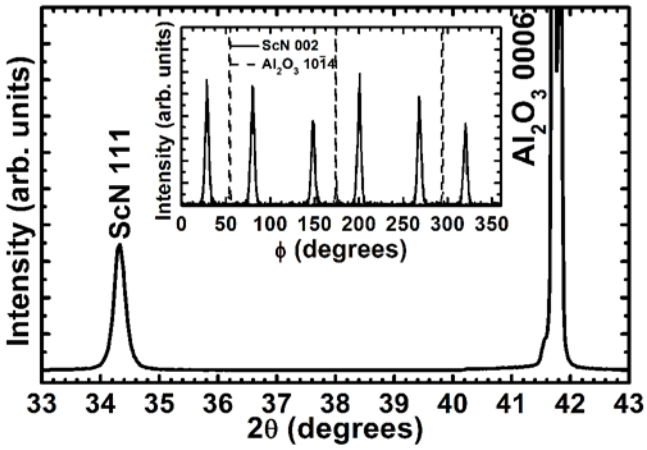
Intensity (arb. units)
ScN 111
Al2O3 0006
2θ (degrees)
33 34 35 36 37 38 39 40 41 42 43
Intensity (arb. units)
ScN 002
Al2O3 10$\bar{1}$4
0 50 100 150 200 250 300 350
ϕ (degrees)

207

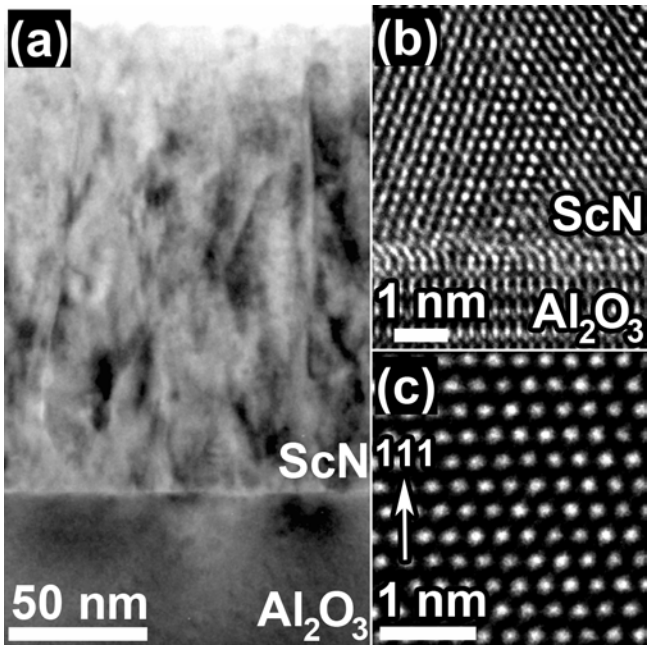

208

209

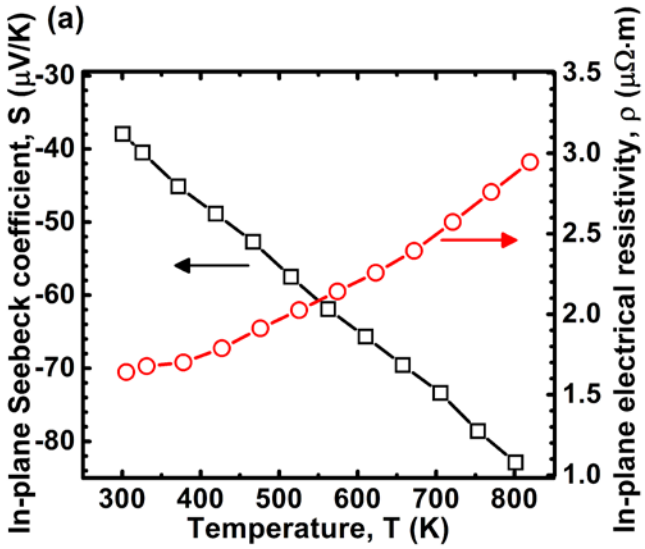
(a)
In-plane Seebeck coefficient, S (μV/K)
In-plane electrical resistivity, ρ (μΩ·m)
Temperature, T (K)
-30
-40
-50
-60
-70
-80
3.5
3.0
2.5
2.0
1.5
1.0
300
400
500
600
700
800

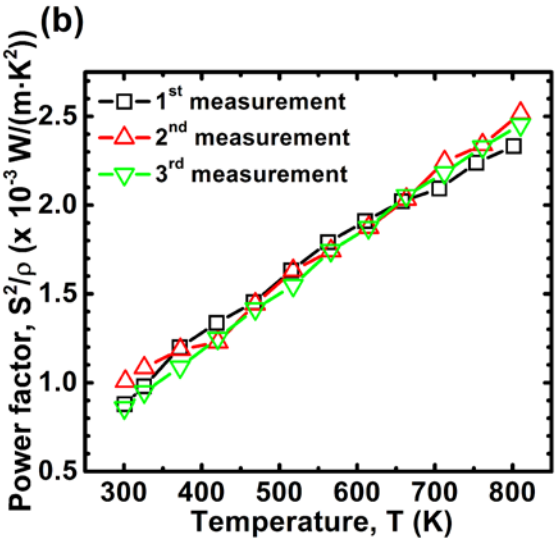
(b)
Power factor, S²/ρ (x 10⁻³ W/(m·K²))
1st measurement
2nd measurement
3rd measurement
Temperature, T (K)
2.5
2.0
1.5
1.0
0.5
300
400
500
600
700
800

210